The 90° Acoustic Spectrum of a High Speed Air Jet

M.E. Goldstein

National Aeronautics and Space Administration

Glenn Research Center

Cleveland, Ohio 44135

Abstract

Tam and Auriault[5] successfully predicted the acoustic spectrum at 90° to the axis of a high speed air jet by using an acoustic equation derived from ad hoc kinetic theory-type arguments. The present paper shows that similar predictions can be obtained by using a rigorous acoustic analogy approach together with actual measurements of the relevant acoustic source correlations. This puts the result on a firmer basis and enables its extension to new situations and to the prediction of sound at other observation angles.

Introduction

The prediction of aircraft exhaust noise continues to be a fruitful area of research. Computational demands still preclude the use of full scale DNS (or even LES[9]) at the high Reynolds numbers and complex geometries of practical interest and the current emphasis remains focused on developing acoustic-analogy type approaches in which the Navier-Stokes equations are rearranged into a form that separates out the linear terms and associates them with propagation effects that can then be determined as part of the calculation. The non-linear terms are treated as "known" source functions to be determined by modeling and, in more recent

approaches, parameterized with the parameters being determined from a steady RANS calculation. The "base" flow (about which the linearization is carried out) is usually assumed to be parallel and the resulting equation is usually referred to as a Lilley's[1] equation.

Most of the early approaches, including the original MGB[2] approach, which neglect variations in retarded time in an appropriate moving frame coordinate system and assume the resulting moving frame correlation tensor to be separable into the product of (usually Gaussian) temporal and spatial components, significantly over-predict both the high and low frequency roll-off of the 90° acoustic spectrum.[4] Tam and Auriault[5] achieved much greater success in this endeavor by using ad hoc kinetic theory type arguments to derive their acoustic equation. However, Morris and Farassat[4] later showed that their result is equivalent to the usual acoustic analogy approach (at least in so far as its predictions of the 90° spectrum are concerned) with the primary difference being in the modeling of the source term, which amounts to assuming a (non-separable) functional form for the second convective derivative of the turbulence correlation that is similar to the functional form used for the turbulence correlation itself in the usual acoustic analogy approaches (but see refs. 30 and 31). Unfortunately, this forces the resulting turbulence spectrum to be singular and therefore incompatible with experimental observations, which would certainly be undesirable in any physics-based theory.

The main purpose of this paper is to show that the Tam and Auriault[5] spectrum can be recovered from an acoustic analogy approach that uses experimentally based (i.e., physically realizable) source modeling together with an appropriate acoustic analogy equation. Reference 6 shows that the Navier-Stokes equations can always be rearranged into the form of the linearized Navier-Stokes equations about a very general "base" flow, but with non-linear dependent variables, with the viscous stresses replaced by a generalized Reynolds stress and with the heat

flux vector replaced by a generalized stagnation enthalpy flux (which would be treated as "known" source strengths when the generalized equations are used as the basis for an acoustic analogy approach). This result leads to a form of Lilley's equation with a modified source term when the "base" flow is taken to be a unidirectional transversely sheared mean flow, i.e., a parallel flow.

It is generally agreed that the enthalpy fluxes, which correspond to the isentropic part of the pressure-density source in the Lighthill approach,[1] are only important for hot jets[1,7,8,28] except, perhaps, at small angles to the downstream jet axis.[10] They are therefore neglected in the present analysis. The resulting equation is solved using a more or less conventional Greens' function approach and the solution is then used to calculate the far field acoustic spectrum. Neglect of the enthalpy and viscous sources are the only approximations introduced at this stage of the analysis, but the results are then simplified by first neglecting variations in retarded time (in an appropriate moving coordinate system[11]) and then introducing an axisymmetric turbulence model.[12–15,3,16] Finally, an empirical turbulent source spectrum, based on recent measurements of Harper-Bourne[17] (in a low Mach number jet) is incorporated into the result and it is shown that the predicted far field acoustic spectrum at 90° to the jet axis is essentially the same as the one proposed by Tam and Auriault.[5]

The Acoustic Analogy Equation and its Far-Field Solution

As indicated in the Introduction, reference 6 shows that the Navier-Stokes equations can be rewritten (for an ideal gas) as the linearized Navier-Stokes equations about a very general "base flow" but with different (in general non-linear) dependent variables, with the heat flux vector replaced by a generalized enthalpy flux and with the viscous stresses replaced by a

generalized Reynolds stress. *This is a true acoustic analogy (in the Lighthill[18,19] sense) in that it shows that there is an exact analogy between the flow fluctuations in any real flow and the linear fluctuations about a very general "base flow" due to an externally imposed "viscous" stress and "heat flux" vector.* When the "base" flow is taken to be the unidirectional transversely sheared mean flow

$$v_i = \delta_{i1}\, U(x_2, x_3),\ \rho = \overline{\rho}(x_2, x_3),$$
$$p = \overline{p} = \text{constant} \qquad (1)$$

where $\boldsymbol{x} = \{x_1, x_2, x_3\}$ is a Cartesian coordinate system, $\boldsymbol{v} = \{v_1, v_2, v_3\}$ denotes the velocity, p the pressure and ρ the density, the general equations reduce to the modified Lilley's[1] equation

$$Lp'_e = \frac{D}{Dt}\left(\frac{\partial}{\partial x_i}\widetilde{c^2}\frac{\partial e'_{ij}}{\partial x_j}\right) - \frac{\partial U}{\partial x_i}\left(2\widetilde{c^2}\frac{\partial^2 e'_{ij}}{\partial x_1 \partial x_j} + (\gamma - 1)\frac{D^2}{Dt^2}e'_{1i}\right) - (\gamma - 1)\frac{D^2}{Dt^2}\frac{\partial \eta'_j}{\partial x_j} \qquad (2)$$

where

$$L \equiv \frac{D}{Dt}\left(\frac{\partial}{\partial x_i}\widetilde{c^2}\frac{\partial}{\partial x_i} - \frac{D^2}{Dt^2}\right) - 2\frac{\partial U}{\partial x_j}\frac{\partial}{\partial x_1}\widetilde{c^2}\frac{\partial}{\partial x_j} \qquad (3)$$

is the variable-density Pridmore-Brown[20] operator

$$\widetilde{c^2} \equiv \gamma\, \overline{p}/\overline{\rho}(x_2, x_3) \qquad (4)$$

is the square of the mean-flow sound speed, γ = the specific heat ratio, t denotes the time,

$$\frac{D}{Dt} \equiv \frac{\partial}{\partial t} + U\frac{\partial}{\partial x_1} \qquad (5)$$

denotes the convective derivative based on U,

$$p'_e \equiv p' + \frac{\gamma - 1}{2}\rho v'_i v'_i \qquad (6)$$

is a generalized pressure fluctuation

$$e'_{ij} \equiv -\rho v'_i v'_j + \frac{\gamma - 1}{2}\delta_{ij}\rho v'^2 + \sigma'_{ij} \qquad (7)$$

is the generalized stress tensor and

$$\eta'_i \equiv -\rho v'_i h'_0 - q'_i + \sigma_{ij} v'_j \qquad (8)$$

is the generalized stagnation enthalpy flux.

Here,

$$v'_i \equiv v_i - \delta_{i1} U \qquad (9)$$

$$h'_o \equiv h' + \frac{1}{2} v'^2 \qquad (10)$$

$$h' \equiv h - \frac{\gamma}{\gamma - 1}\frac{\overline{p}}{\overline{\rho}} \qquad (11)$$

denote fluctuating quantities with h being the enthalpy and σ'_{ij} and q_i' being the fluctuating viscous stress and heat flux vector, respectively, which are believed to play a negligible direct role in the sound generation process[18,19] and are therefore neglected in the following. The fluctuating enthalpy flux η_i' will also be neglected since, as noted in the Introduction, this quantity is generally considered to be unimportant for cold jets[1,7,8]—except perhaps at small angles to the downstream axis.[10]

Then eq. (2) can be formally solved in terms of the free space Greens' function[21] $G(\boldsymbol{x}, t | \boldsymbol{y}, \tau)$, which satisfies

$$LG(\boldsymbol{x}, t | \boldsymbol{y}, \tau) = \delta(\boldsymbol{x} - \boldsymbol{y})\delta(t - \tau) \qquad (12)$$

and has outgoing wave behavior at infinity, to obtain the following expression

$$\overline{p^2}(\boldsymbol{x},t_o) = \int_{-\infty}^{\infty} \iiint_V \overline{\gamma}_{ijkl}(\boldsymbol{x}|\boldsymbol{y};\boldsymbol{\eta},t_o+\tau_o) \times R_{ijkl}(\boldsymbol{y};\boldsymbol{\eta},\tau_o)\,d\boldsymbol{y}\,d\boldsymbol{\eta}\,d\tau_o \qquad (13)$$

for the pressure autocovariance[22] (notice that p_e' reduces to p' in the far field)

$$\overline{p^2}(\boldsymbol{x},t_o) \equiv \frac{1}{2T}\int_{-T}^{T} p_e'(\boldsymbol{x},t)p_e'(\boldsymbol{x},t+t_o)\,dt \qquad (14)$$

where V denotes integration over all space, T denotes some large but finite time interval, the propagation factor $\overline{\gamma}_{ij}(\boldsymbol{x},t|\boldsymbol{y},\tau)$ is defined in appendix A and

$$R_{ijkl}(\boldsymbol{y};\boldsymbol{\eta},\tau_o) \equiv \frac{1}{2T}\int_{-T}^{T} \rho v_i' v_j'(\boldsymbol{y},\tau) \rho v_k' v_l'(\boldsymbol{y}+\boldsymbol{\eta},\tau+\tau_o)\,d\tau \qquad (15)$$

is the density-weighted, fourth-order, two-point, time-delayed fluctuating velocity correlation- with the indicated arguments referring to all three terms preceding the parentheses. The details are given in appendix A.

Lighthill[18,19] pointed out that acoustic predictions tend to be less dependent on the detailed structure of the turbulence when variations in retarded time across the correlation volume $\Delta\boldsymbol{\eta}$ can be neglected, which is a reasonable approximation in a reference frame

$$\boldsymbol{\xi} \equiv \boldsymbol{\eta} - \hat{\mathbf{i}}U_c\tau_o \qquad (16)$$

moving with the local convection velocity, $U_c(\mathbf{y})$,of the turbulence. Ffowcs Williams[11] showed that this idea is best implemented by introducing the moving frame correlation tensor

$$R_{ijkl}^M(\boldsymbol{y};\boldsymbol{\xi},\tau_0) \equiv R_{ijkl}(\boldsymbol{y};\boldsymbol{\xi}+\hat{\mathbf{i}}U_c\tau_o,\tau_o) \qquad (17)$$

into the relevant pressure autocovariance formula (eq. (13) in our case) to obtain

$$\overline{p^2(\boldsymbol{x},t_o)} = \int_{-\infty}^{\infty}\iiint_V \overline{\gamma}_{ijkl}\left(\boldsymbol{x}\middle|\boldsymbol{y};\boldsymbol{\xi}+\hat{\mathbf{i}}U_c\tau_0,t_o+\tau_o\right) R^M_{ijkl}(\boldsymbol{y};\boldsymbol{\xi},\tau_o)\,d\boldsymbol{y}\,d\boldsymbol{\xi}\,d\tau_o \qquad (18)$$

Our interest is in the far field spectrum

$$I_\omega(\boldsymbol{x}) \equiv \frac{1}{2\pi}\int_{-\infty}^{\infty} e^{i\omega t_o}\,\overline{p^2}(\boldsymbol{x},t_o)\,dt_o \qquad (19)$$

which can, in principle, be calculated by taking the Fourier transform of eq. (18) and using the convolution theorem.[21] Unfortunately, this cannot be done in practice because the Fourier transform of $R_{ijkl}(\boldsymbol{y};\boldsymbol{\eta},\tau_o)$, and therefore of $R^M_{ijkl}(\boldsymbol{y};\boldsymbol{\xi},\tau_0)$, does not exist[16] (see p.179). This difficulty can be overcome by replacing $R_{ijkl}(\boldsymbol{y};\boldsymbol{\eta},\tau_o)$ with $R_{ijkl}(\boldsymbol{y};\boldsymbol{\eta},\tau_o) - R_{ij}(\boldsymbol{y};\mathbf{0},0)R_{kl}(\boldsymbol{y}+\boldsymbol{\eta};\mathbf{0},0)$ where $R_{ij}(\boldsymbol{y};\boldsymbol{\eta},\tau_0)$ is defined by eq. (30). This does not change the radiated sound because $R_{ij}(\boldsymbol{y};\mathbf{0},0)R_{kl}(\boldsymbol{y}+\boldsymbol{\eta};\mathbf{0},0)$ is steady and, therefore produces no sound. It then follows that

$$I_\omega(\boldsymbol{x}|\boldsymbol{y}) = 2\pi\int_{-\infty}^{\infty}\int_V \Gamma_{ij}(\boldsymbol{x}|\boldsymbol{y};\omega)\Gamma^*_{kl}\left(\boldsymbol{x}\middle|\boldsymbol{y}+\boldsymbol{\xi}+\hat{\boldsymbol{i}}U_c\tau_o;\omega\right)e^{-i\omega\tau_o}R^M_{ijkl}(\boldsymbol{y},\boldsymbol{\xi},\tau_o)\,d\boldsymbol{\xi}\,d\tau_o \qquad (20)$$

where

$$\Gamma_{ij} \equiv \frac{1}{2\pi}\int_{-\infty} e^{i\omega(t-\tau)}\gamma_{ij}(\boldsymbol{x}|\boldsymbol{y},t-\tau)\,d(t-\tau) \qquad (21)$$

is the Fourier transform of γ_{ij} (we use capital letters to denote Fourier transform of the corresponding lower case quantity) and we introduced $I_\omega(\boldsymbol{x}\,|\,\boldsymbol{y})$,the acoustic spectrum at $\boldsymbol{x}$ due to a unit volume of turbulence at $\boldsymbol{y}$, i.e.,

$$I_\omega(\boldsymbol{x}) = \int_V I_\omega(\boldsymbol{x}|\boldsymbol{y})\,d\boldsymbol{y} \qquad (22)$$

in order to simplify the formulas.[22] The relevant far field expansion of Γ_{ij} is given in appendix B.

The only approximation made up to this point is the neglect of the enthalpy and viscous source terms, but eq. (20) will depend on the turbulent source correlations only through

$$\mathcal{R}_{ijkl}(\boldsymbol{y},\tau_o) \equiv \int_V R^M_{ijkl}(\boldsymbol{y},\xi,\tau_o)\,d\boldsymbol{\xi} \qquad (23)$$

if variations in retarded time across the correlation volume are neglected, i.e., if $\Gamma^*_{kl}\left(\boldsymbol{x}\middle|\boldsymbol{y}+\boldsymbol{\xi}+\hat{\boldsymbol{i}}U_c\tau;\omega\right)$ is assumed to be constant over the correlation volume.[11] However, the definition (17) implies that the integration variable in eq. (23) can be changed back to $\boldsymbol{\eta}$, which means that

$$\mathcal{R}_{ijkl}(\boldsymbol{y},\tau_o) \equiv \int_V R_{ijkl}(\boldsymbol{y},\boldsymbol{\eta},\tau_o)\,d\boldsymbol{\eta} \qquad (24)$$

i.e., the source correlation can be expressed in either the fixed or moving frame once the retarded time is neglected. (But introduction of the moving frame is necessary in order to get the correct τ_0-dependence in Γ^*_{kl}.)

Equation (20) can now be written more simply as

$$I_\omega(\boldsymbol{x}|\boldsymbol{y}) \to \left(\frac{2\pi}{x}\right)^2 \frac{2\pi\omega}{c_\infty}\sin\theta\,\bar{\Gamma}_{ij}(\boldsymbol{x}|\boldsymbol{y}_\perp)\bar{\Gamma}^*_{kl}$$
$$(\boldsymbol{x}|\boldsymbol{y}_\perp)\Phi^*_{ijkl}\left(\boldsymbol{y};\omega(1-M_c\cos\theta)\right)\text{as } x\to\infty \qquad (25)$$

where

$$\Phi_{ijkl}(\boldsymbol{y},\omega) \equiv \frac{1}{2\pi}\int_{-\infty}^{\infty} e^{i\omega\tau_o}\mathcal{R}_{ijkl}(\boldsymbol{y},\tau_o)\,d\tau_o \qquad (26)$$

is the spectral tensor of the source correlation and

$$M_c \equiv U_c / c_\infty \qquad (27)$$

is the convective Mach number of the turbulence. This result shows that it is only necessary to model the overall spectral tensor itself and not the detailed two-point time delayed correlations of the turbulence. However, the radiated sound should still be relatively insensitive to the detailed turbulence structure even when the latter quantities are modeled (as is at least partially done below). This would not be the case if the moving frame had not been introduced before neglecting the retarded time variations.[11,22]

Our interest here is in the spectrum at 90° to the jet axis where $\cos\theta = 0$. Appendix B shows that

$$I_\omega(\boldsymbol{x}|\boldsymbol{y}) = \frac{(\omega/c_\infty)^4}{(4\pi x)^2}\left[\frac{x_i x_j}{x^2} - \frac{\gamma-1}{2}\delta_{ij} + \frac{i(\gamma-1)\delta_{1i}}{\omega}\frac{\partial U}{\partial y_j}\right]\left[\frac{x_k x_l}{x^2} - \frac{\gamma-1}{2}\delta_{kl} - \frac{i(\gamma-1)}{\omega}\delta_{1k}\frac{\partial U}{\partial y_l}\right]\Phi^*_{ijkl}(\boldsymbol{y};\omega)$$
$$\text{for } \theta = \pi/2. \qquad (28)$$

when $\widetilde{c_0^2} = c_\infty^2 = \text{constant}$, i.e., in the isothermal case.

The Quasi-Normal and Axisymmetric Turbulence Approximations

To proceed further, we need to know something about the source spectral tensor Φ_{ijkl}. The usual approach[12,13,3] is to begin by assuming that the turbulence is quasi-normal[16] (see ref. 10) in order to obtain some relations among its components. It then follows that (see comments preceding eq. (20)).

$$R_{ijkl}\left(y;\boldsymbol{\eta},\tau_o\right) = R_{ik}\left(y;\boldsymbol{\eta},\tau_o\right)R_{jl}\left(y;\boldsymbol{\eta},\tau_o\right) + R_{il}\left(y;\boldsymbol{\eta},\tau_o\right)R_{jk}\left(y;\boldsymbol{\eta},\tau_o\right) \qquad (29)$$

where

$$R_{ij}\left(\boldsymbol{y};\boldsymbol{\eta},\tau_o\right) \equiv \frac{1}{2T}\int_{-T}^{T}\sqrt{\rho}v_i'\left(\boldsymbol{y},\tau\right)\sqrt{\rho}v_j' \left(\boldsymbol{y}+\boldsymbol{\eta},\tau+\tau_o\right)d\tau \qquad (30)$$

is the second order correlation. To further reduce the number of independent components it is usual to assume some kinematically possible symmetric form for the second order correlations. Early studies[23] assumed the turbulence to be isotropic, but that turns out to be incompatible with the Harper-Bourne[17] measurements that will be introduced below. The simplest assumption compatible with his results is the one introduced in references 12 and 13, namely that the turbulence is axisymmetric which implies that[16]

$$R_{ij}\left(\boldsymbol{y};\boldsymbol{\eta},\tau_o\right) = A_0\eta_i\eta_j + B_0\delta_{ij} + C_0\delta_{1i}\delta_{1j} + D_0\left(\delta_{1j}\eta_j + \delta_{1j}\eta_i\right) \qquad (31)$$

where A_0, B_0, C_0, and D_0 are functions of $\boldsymbol{y}$, τ_0, and $\eta_\perp$; A_0, B_0 and C_0 are even functions $\eta_\perp$ and D_0 is an odd function of this quantity. This model is chosen because it is the most general of those whose mathematical properties have been studied in the literature and because it reflects the fact that the cross flow velocity components tend to be much more similar to one another

than to the stream-wise component—even for non-axisymmetric flows. Inserting eq. (31) into eq. (29) and inserting the result into eq. (25) via eqs. (24) and (26) yields (after a straight forward but tedious calculation that follows along the lines of the one in appendix A of reference 12)

$$I_\omega\left(\boldsymbol{x}|\mathbf{y}\right)(4\pi x)^2 = 2\left(\frac{\omega}{c_\infty}\right)^4 \left[\Phi_1 - (\gamma-1)\Phi_2 + \left(\frac{\gamma-1}{2}\right)^2 \Phi_3\right] + \left[(\gamma-1)\frac{\omega}{c_\infty}\left|\nabla M\right|\right]^2 \Phi_4 \qquad (32)$$

where

$$\Phi_1 \equiv \frac{1}{2\pi}\int_{-\infty}^{\infty} e^{-i\omega\tau_o}\int_V R_{22}^2\left(\boldsymbol{y},\boldsymbol{\eta},\tau_o\right)d\boldsymbol{\eta}\, d\tau_o \qquad (33a)$$

$$\Phi_2 \equiv \frac{1}{2\pi}\int_{-\infty}^{\infty} e^{-i\omega\tau_o}\int_V \left(R_{23}^2 + R_{12}^2 + R_{22}^2\right)d\boldsymbol{\eta}\, d\tau_o \qquad (33b)$$

$$\Phi_3 \equiv \frac{1}{2\pi}\int_{-\infty}^{\infty} e^{-i\omega\tau_o}\int_V \left(4R_{12}^2 + 2R_{23}^2 + R_{11}^2 + 2R_{22}^2\right)d\boldsymbol{\eta}\, d\tau_o \qquad (33c)$$

and

$$\Phi_4 \equiv \frac{1}{2\pi}\int_{-\infty}^{\infty} e^{-i\omega\tau_o}\int_V \left(R_{12}{}^2 + R_{11}R_{22}\right)d\boldsymbol{\eta}\, d\tau_o \qquad (33d)$$

are seemingly independent spectral functions. However, the coefficients A_0, B_0, C_0, and D_0 are not all independent and when compressibility effects are neglected (i.e., when ρ is treated as a constant) these turbulence correlations can be expressed in terms of two independent scalar functions of $\boldsymbol{y}$, τ_0, $\eta_\perp$, and η_1, say *a* and *b,* both of which are even functions of the latter variable.[14,15,24] The resulting expressions for the two point correlations are given in appendix C,

where they are used to express the integrals over V in eq. (33) in terms of *a* and *b*. Equations (C–1) to (C–4) suggest that these latter quantities will scale like

$$b = \widetilde{\rho u_1^2} B\left(\tilde{\eta}_\perp, \tilde{\eta}_1\right) L_\perp^2 / 2 \qquad (34)$$

and

$$g \equiv a - b_{\eta_1\eta_1} = \widetilde{\rho u_2^2} D\left(\tilde{\eta}_\perp, \tilde{\eta}_1\right) \qquad (35)$$

where

$$\tilde{\eta}_1 \equiv \eta_1 / L_1 \qquad (36)$$

$$\tilde{\eta}_\perp \equiv \eta_\perp / L_\perp \qquad (37)$$

L_1 and $L_\perp$ denote characteristic stream-wise and transverse length scales of the turbulence, *B* and *D* are *O(1)* functions of the indicated arguments,

$$\widetilde{\rho u_1^2} \equiv R_{11}\left(\boldsymbol{0}, 0\right) \qquad (38)$$

and

$$\widetilde{\rho u_2^2} \equiv R_{22}\left(\boldsymbol{0}, 0\right) \qquad (39)$$

Turbulence measurements suggest that

$$\varepsilon \equiv \frac{L_\perp}{4L_1} \qquad (40)$$

ought to be small. In fact, Harper-Bourne's[17] measurements (to be discussed below) suggest that $\varepsilon \simeq 2.7\times10^{-2}$. The scalings (34) through (40) are inserted into eqs. (C–5) through (C–9) of appendix C where it is shown that

$$\frac{\left(4/3\right)\Phi_1}{2\pi L_1 L_\perp^2 \left(\widetilde{\rho u_1^2}\right)^2} = \frac{\Phi_2}{2\pi L_1 L_\perp^2 \left(\widetilde{\rho u_1^2}\right)^2}$$

$$= r^2 \int_{-\infty}^{\infty} e^{-i\omega\tau_0} \int_{-\infty}^{\infty}\int_{0}^{\infty}\left(\tilde{\eta}_\perp \frac{\partial D}{\partial \tilde{\eta}_\perp}\right)^2 \tilde{\eta}_\perp d\tilde{\eta}_\perp d\tilde{\eta}_1 d\tau_0 \quad (41a,b)$$

$$\frac{\Phi_3}{2\pi L_1 L_\perp^2 \left(\widetilde{\rho u_1^2}\right)^2} = \int_{-\infty}^{\infty} e^{-i\omega\tau_0} \int_{-\infty}^{\infty}\int_{0}^{\infty}\left[\frac{\bar{B}^2}{8} + 2r^2\left(\tilde{\eta}_\perp \frac{\partial D}{\partial \tilde{\eta}_\perp}\right)^2\right]$$

$$\tilde{\eta}_\perp d\tilde{\eta}_\perp d\tilde{\eta}_1 d\tau_0 \quad (41c)$$

$$\frac{\Phi_4}{2\pi L_1 L_\perp^2 \left(\widetilde{\rho u_1^2}\right)^2}$$

$$= \frac{r}{2}\int_{-\infty}^{\infty} e^{-i\omega\tau_0} \int_{-\infty}^{\infty}\int_{0}^{\infty} \bar{B}\frac{\partial}{\partial \tilde{\eta}_\perp}\left(\tilde{\eta}_\perp{}^2 D\right) d\tilde{\eta}_\perp d\tilde{\eta}_1 d\tau_0 \quad (41d)$$

when $O\left(\varepsilon^2\right)$ terms are neglected-the ratio r is defined by

$$r \equiv \widetilde{\rho u_2^2} \Big/ \widetilde{\rho u_1^2} \quad (42)$$

and $\bar{B}$ is given by eq.(C–14).

Lacking any specific data to the contrary, it seems reasonable to suppose that

$$\Phi_0 \equiv \frac{1}{\pi}\int_{-\infty}^{\infty} e^{-i\omega\tau_o} \int_V R_{11}^2\left(\boldsymbol{y}, \boldsymbol{\eta}, \tau_o\right) d\boldsymbol{\eta}\, d\tau_o$$

$$= \frac{1}{(\Gamma r)^2}\frac{1}{\pi}\int_{-\infty}^{\infty} e^{-i\omega\tau_o} \int_V R_{22}^2\left(\boldsymbol{y}, \boldsymbol{\eta}, \tau_o\right) d\boldsymbol{\eta}\, d\tau_o \quad (43)$$

Equation (32) then becomes

$$I_\omega\left(\mathbf{x}|\mathbf{y}\right)\left(2\pi x c_\infty\right)^2$$

$$= C_0^2 \Phi_o\left(\boldsymbol{y},\omega\right)\left(\frac{\omega}{c_\infty}\right)^2\left[\omega^2+\left(U_c\kappa\right)^2\right] \qquad (44)$$

where Γ and, therefore,

$$2C_0^2 \equiv \frac{2}{3}(\Gamma r)^2$$

$$\left[\frac{3}{4}-(\gamma-1)+2\left(\frac{\gamma-1}{2}\right)^2\right]+\frac{1}{2}\left(\frac{\gamma-1}{2}\right)^2 \qquad (45)$$

are constants, i.e., independent of ω, and

$$\kappa \equiv \left(\frac{\gamma-1}{2}\right)\frac{|\nabla U|}{U_c C_0}$$

$$\sqrt{\frac{2r\int_{-\infty}^{\infty} e^{-i\omega\tau_0}\int_{-\infty}^{\infty}\int_{0}^{\infty}\bar{B}\left(\frac{\partial}{\partial\tilde{\eta}_\perp}\tilde{\eta}_\perp{}^2 D\right)d\tilde{\eta}_\perp d\tilde{\eta}_1 d\tau_0}{\int_{-\infty}^{\infty} e^{-i\omega\tau_0}\int_{-\infty}^{\infty}\int_{0}^{\infty}\bar{B}^2\tilde{\eta}_\perp d\tilde{\eta}_\perp d\tilde{\eta}_1 d\tau_0}} \qquad (46)$$

The Harper-Bourne Spectrum

The results can not be made more explicit without inputting more specific information about the turbulence structure. This is accomplished with the aid of some recent measurements[17] of the two point fourth order stream-wise velocity correlation spectra along the centerline of the mixing layer in a low Mach number jet, which would most closely correspond to

$$H_o\left(\boldsymbol{y},\boldsymbol{\eta},\omega\right) \equiv \frac{1}{\pi}\int_{-\infty}^{\infty} e^{-i\omega\tau_o} R_{11}^2\left(\boldsymbol{y},\boldsymbol{\eta},\tau_o\right)d\tau_o \qquad (47)$$

with the quasi-normal approximation that is being used in the present analysis.

Harper-Bourne[17] divided H_0 into the three components (see his eq. (2.5) and (2.7) on p. 2)

$$H_o = H_o\left(\boldsymbol{y},\mathbf{0},\omega\right) R\left(\boldsymbol{y},\frac{\eta_1}{l_1},\frac{\eta_\perp}{l_\perp},\omega\right) e^{i\omega\tau_p} \quad (48)$$

where l_1, $l_\perp$ are the spectral stream-wise and transverse length scales (not necessarily the same as the time domain length scales L_1 and $L_\perp$ introduced above) and

$$\tau_p \simeq \frac{\eta_1}{U_c} \quad (49)$$

No assumption is made about the decomposition of the correlations into products of their space and time components with this approach.

The first factor can be evaluated from his measurements of $R_{1111}\left(\mathbf{y},\mathbf{0},\tau_0\right)$, which are well represented by the exponential $e^{-\lambda|\tau_o|}$ -implying that

$$H_o\left(\boldsymbol{y},\mathbf{0},\omega\right) = \frac{\lambda\rho^2\widetilde{u_1^4}}{\pi\left(\lambda^2+\omega^2\right)} \quad (50)$$

Inserting these into eq. (43) and using the result in eq. (44) shows that

$$I_\omega\left(\mathbf{x}|\mathbf{y}\right) = C_0^2 \frac{\lambda\rho\widetilde{u_1^4}\left[\omega^2+\left(U_c\kappa\right)^2\right]}{x^2 c_\infty^4(\lambda^2+\omega^2)\omega} \times 2U_c^3\bar{l}_1\bar{l}_\perp^2\bar{R}\left(\boldsymbol{y},\bar{l}_1\right) \quad (51)$$

where

$$\bar{R}\left(\boldsymbol{y},\bar{l}_1\right) \equiv 2\pi\int_{-\infty}^{\infty}\int_{0}^{\infty} R\left(\boldsymbol{y},\bar{\eta}_1,\bar{\eta}_\perp\right)e^{-2\pi i\bar{\eta}_1\bar{l}_1}d\bar{\eta}_1\bar{\eta}_\perp d\bar{\eta}_\perp \quad (52)$$

and $\bar{l}_1$ and $\bar{l}_\perp$ are defined by

$$\bar{l}_1 \equiv \frac{\omega l_1}{2\pi U_c} \qquad (53)$$

and

$$\bar{l}_\perp \equiv \frac{\omega l_\perp}{2\pi U_c} \qquad (54)$$

Harper-Bourne's measurements seem to indicate that $R\left(\boldsymbol{y}, \bar{\eta}_1, \omega\right)$ behaves like $e^{-|\bar{\eta}_1|}$, which, as pointed out by Khavaran et al.,[27] is inconsistent with Hinze's[24] parabolic vertex requirement. We therefore apply a Gaussian filter to his measured value of *R*, say R_m, to obtain

$$R\left(\boldsymbol{y}, \bar{\eta}_1, \bar{\eta}_\perp\right) = \frac{\int_{-\infty}^{\infty} e^{-\left(\frac{\bar{\eta}_1 - \hat{\eta}_1}{2\beta}\right)^2} R_m\left(\boldsymbol{y}, \hat{\eta}_1, \bar{\eta}_\perp\right) d\hat{\eta}_1}{\sqrt{\pi}\, e^{\left(\beta/l_1\right)^2} \operatorname{erfc.}\left(\beta/l_1\right)} \qquad (55)$$

which smoothes out the cusp at $\bar{\eta}_1 = 0$ but, otherwise behaves similarly to R_m (note the data scatter around η_1 = 0 in Harper-Bourne's fig. 14(a)). The Error function factor, $e^{\left(\beta/l_1\right)^2} \operatorname{erfc.}\left(\beta/l_1\right)$, has been inserted in the denominator in order to insure that *R* still satisfies the normalization condition, $R\left(\boldsymbol{y}, 0, 0\right)$ = 1, when $R_m\left(\boldsymbol{y}, \bar{\eta}_1, 0\right) = e^{-|\bar{\eta}_1|}$. In fact it is easy to show more generally that, with this choice of $R_m\left(\boldsymbol{y}, \bar{\eta}_1, 0\right)$,

$$R\left(\boldsymbol{y}, \bar{\eta}_1, 0\right) = \frac{e^{-\bar{\eta}_1} \operatorname{erfc.}\left(\frac{\beta}{l_1} - \frac{\bar{\eta}_1 l_1}{2\beta}\right) + e^{\bar{\eta}_1} \operatorname{erfc.}\left(\frac{\beta}{l_1} + \frac{\bar{\eta}_1 l_1}{2\beta}\right)}{2 \operatorname{erfc.}\left(\beta/l_1\right)} \qquad (56)$$

which behaves like $e^{-|\bar{\eta}_1|}$ for large η_1 but has continuous slope at $\eta_1 = 0$.

Inserting eq. (55) into eq. (52), using the convolution theorem, and inserting the result into eq. (51) yields

$$I_\omega\left(\mathbf{x}|\mathbf{y}\right) = C_0^2 \frac{\lambda\rho\widetilde{u_1^4} e^{-(\beta\omega/U_c)^2}\left[\omega^2 + \left(U_c\kappa\right)^2\right] 2U_c^3 \bar{l}_1 \bar{l}_\perp^2 \bar{R}_m\left(\boldsymbol{y}, \bar{l}_1\right)}{x^2 c_\infty^4 \exp.\left(\beta/l_1\right)^2 \operatorname{erfc}.\left(\beta/l_1\right)(\lambda^2+\omega^2)\omega} \tag{57}$$

where

$$\bar{R}_m\left(\boldsymbol{y}, \bar{l}_1\right) \equiv 2\pi \int_{-\infty}^{\infty} \int_{0}^{\infty} R_m\left(\boldsymbol{y}, \bar{\eta}_1, \bar{\eta}_\perp\right) e^{-2\pi i \bar{\eta}_1 \bar{l}_1} d\bar{\eta}_1 \bar{\eta}_\perp d\bar{\eta}_\perp \tag{58}$$

which reduces to eq. (51) when $\beta = 0$.

Comparison with the Tam and Auriault result

The form

$$R_m = e^{-\bar{\eta}_\perp^2} e^{-|\bar{\eta}_1|} \tag{59}$$

agrees fairly well with Harper-Bourne's measurements when $\eta_1 = 0$ and $\eta_\perp \neq 0$ and also when $\eta_\perp = 0$ and $\eta_1 \neq 0$. Inserting this into eq. (58), integrating over $\boldsymbol{\eta}$ and inserting the result into eq. (57) shows that

$$I_\omega\left(\mathbf{x}|\mathbf{y}\right)$$

$$= C_0^2 \frac{\lambda\rho\widetilde{u_1^4} e^{-(\beta\omega/U_c)^2} 2U_c^5 \overline{l}_1 \overline{l}_\perp^2 \kappa^2}{x^2 c_\infty^4 \exp.\left(\beta/l_1\right)^2 \operatorname{erfc}.\left(\beta/l_1\right)(\lambda^2+\omega^2)\omega} \left[\frac{1+\left(\omega/U_c\kappa\right)^2}{1+\left(2\pi\overline{l}_1\right)^2}\right] \qquad (60)$$

The form (59) is consistent with the assumption that $B/2 = D = \overline{a}\left(\overline{\eta}_1, \tau_o\right) e^{-\overline{\eta}_\perp^2/2}$ when l_1 and $l_\perp$ are taken to be constants (i.e., independent of ω), which then implies that the ratio of integrals in eq. (46) is equal to ½ and that $\Gamma^2 = 3$ in eq. (43). So that for r = ½, γ = 1.4, and U_c = 0.65 U_J

$$\kappa \approx \frac{|\nabla U|}{2U_J} \approx \frac{1}{2 l_s D_J} \qquad (61)$$

where $l_s \approx 0.345$ denotes the characteristic length scale of the mean velocity divided by the jet diameter D_J. Harper-Bourne's measurements show that $l_\perp$ and l_1 are relatively constant and that the latter can be approximated by $l_1 \approx .691 D_J$ at sufficiently low frequencies. It therefore follows that the square bracket in eq. (60) is approximately equal to unity, which means that the resulting 90° acoustic spectrum should be of the form

$$I_\omega\left(\mathbf{x}|\mathbf{y}\right) \propto \frac{e^{-(\beta\omega/U_c)^2}\omega^2}{\left(\omega^2+\lambda^2\right)} \qquad (62)$$

which is the same as the spectral form proposed by Tam and Auriault,[5] who take $\frac{\beta l_1}{U_c} = \frac{c_l}{2\varepsilon}\frac{k^{3/2}}{\bar{u}}$ and $\lambda = \varepsilon/c_\tau k$ (see eq. (53) of ref. 4) where c_l and c_τ adjustable constants and k and ε (not to be confused with the ε in eq. (40)) are determined from a k-ε RANS calculation. Notice that this result behaves like ω^2 as $\omega \to 0$ and converges like $e^{-(\beta\omega/U_c)^2}$ as $\omega \to \infty$.

However, Harper-Bourne demonstrates that the separable form (59) does not work at oblique separations where η_1 and $\eta_\perp$ are both non-zero and, more importantly, his fig. 13 shows that l_1 and $l_\perp$ are only constant at relatively low frequencies with the scaled length scales $\bar{l}_i$ and $\bar{l}_\perp$ becoming constant as $\omega \to \infty$. It, therefore, follows from eq. (57) and the asymptotic behavior of the Error function (ref. 29, p. 298 #7.1.23) that $I_\omega(\boldsymbol{x}|\boldsymbol{y})$ converges like $e^{-(\beta\omega/U_c)^2}$ when $\kappa \approx const.$ and $\omega \to \infty$, i.e., it has the same high frequency behavior as Tam and Auriault result (62). The general formula (57) therefore coincides with that result at both high and low to moderately-low frequencies-even with frequency dependent length scales.

The two results differ at intermediate to moderately high frequencies by the factor

$$\frac{\exp.\left(\beta/l_1^{(0)}\right)^2 \operatorname{erfc}.\left(\beta/l_1^{(0)}\right)}{\exp.\left(\beta/l_1\right)^2 \operatorname{erfc}.\left(\beta/l_1\right)} \times \left[\frac{1+\left(\omega/U_c\kappa\right)^2}{1+\left(2\pi\bar{l}_1\right)^2}\right]\left(\frac{l_1}{l_1^{(0)}}\right)^2\left(\frac{l_\perp}{l_\perp^{(0)}}\right) \qquad (63)$$

(where $l_1^{(0)} = .691 D_J$ and $l_\perp^{(0)}$ are the initial constant values of l_1 and $l_\perp$), which is no longer equal to unity at these frequencies but becomes constant as $\omega \to \infty$. On the other hand,

Khavaran et al.[27] point out that the Tam and Auriault[5] data comparisons do not account for atmospheric attenuation. Figure 1 (taken, in part, from ref. 27) shows that the latter comparisons (curve 2) under predict the high frequency portion of the spectrum for a Mach number 0.5 cold jet when atmospheric absorption effects are included. But multiplying the result shown in curve 2 (which involves a summation over the jet) by the overall (or average) correction factor (63) (with l_1 and $l_\perp$ given by the formulas in Harper-Bourne's fig.13), which is hopefully relatively independent of the choice of source point, leads to curve 1, which is in much better agreement with the data. It would, of course, be better to sum the actual formula (57) over the jet with appropriate local values for the parameters, but since the measurements are all at a single location, this does not seem to be warranted at the present time.

Harper-Bourne obtains the best fit to his data with the non-separable form

$$R_m = e^{-\sqrt{\bar{\eta}_1^2+\bar{\eta}_\perp^4}} \qquad (64)$$

which can be inserted into eq. (57) via eq. (58) to obtain

$$I_\omega(\mathbf{x}|\mathbf{y}) = C_0^2 \frac{\lambda\rho\tilde{u}_1^4 e^{-(\beta\omega/U_c)^2}\left[\omega^2+(U_c\kappa)^2\right]}{x^2 c_\infty^4\left(\exp.\left(\beta/l_1\right)^2\operatorname{erfc}.\left(\beta/l_1\right)\right)(\lambda^2+\omega^2)\omega\left[1+(2\pi\bar{l}_1)^2\right]^{3/2}} \times \pi U_c^3 \bar{l}_1 \bar{l}_\perp^2 \qquad (65)$$

which has the same high and low frequency behavior as eq. (60) but is slightly different from it at intermediate frequencies. More in depth data comparisons may be needed to determine if this result will provide a better representation of the data.

Discussion

As noted in the Introduction, Morris and Farassat[4] argue that, for the same mean flow calculation, the Tam and Auriault result (62) yields a better prediction of the 90° acoustic spectrum than methods based on the usual acoustic analogy approximations. They also show that this type of spectrum can be obtained within the acoustic analogy frame work if the usual source modeling is applied to $\frac{D^2}{D\tau_o^2} R_{ijkl}$ rather than to R_{ijkl} as was done above. But this would imply that the R_{ijkl} spectrum becomes infinite like ω^{-2} as $\omega \to 0$, which is certainly not consistent with experimental results. The conventional acoustic analogy approach leads to a multiplicative factor of ω^4 in the spectrum[22] (rather than the ω^2 factor in eq. (62)) due to the quadrupole nature of the source). The ω^2 factor is characteristic of a dipole source. In the present approach, the energy equation introduces the dipole type source term $-\frac{\partial U}{\partial x_i}(\gamma - 1)\frac{D^2}{Dt^2} e'_{1i}$ in the acoustic analogy eq. (2) which combines with the quadrupole source and a portion of the physically realizable spectral function (eq. (48)) that arises from the non-separable nature of the source to produce the correct spectral form.

It is important to keep in mind that while the 90° spectrum is useful from a diagnostics point of view, the maximum acoustic intensity occurs at relatively small angles to the downstream axis for most (if not all) high speed air jets. The predictions of the present model would differ from the Tam and Auriault[5] results at these angles or, for that matter, from any modification of the conventional acoustic analogy.

Acknowledgement

The author would like to thank Drs. Abbas Khavaran and Stewart Leib for their helpful comments.

Appendix A

The Pressure Autocovariance

The formal Green's function solution to eq. (2) can be written as

$$p_e'(\boldsymbol{x},t) = \int_V \int_{-\infty}^{\infty} \rho v_i' v_j' \gamma_{ij}(\boldsymbol{x},t|\boldsymbol{y},\tau)\, d\mathbf{y}\, d\tau \qquad (A-1)$$

where $\rho v_i' v_j'$ is evaluated at $\boldsymbol{y},\tau$,

$$\gamma_{ij}(\boldsymbol{x},t|\boldsymbol{y},\tau) \equiv \left[\left(\delta_{in}\delta_{jm} - \frac{\gamma-1}{2}\delta_{ij}\delta_{nm} \right) \right.$$
$$\left(\frac{\partial}{\partial y_m}\widetilde{c^2}\frac{\partial}{\partial y_n}\frac{D}{D\tau} + 2\frac{\partial}{\partial y_m}\widetilde{c^2}\frac{\partial U}{\partial y_n}\frac{\partial}{\partial y_1} \right)$$
$$\left. + \delta_{1i}(\gamma-1)\frac{\partial U}{\partial y_j}\frac{D^2}{D\tau^2} \right] G(\boldsymbol{x},t|\boldsymbol{y},\tau) \qquad (A-2)$$

where all the terms in square brackets are part of the differential operator and we have integrated by parts to transfer the derivatives from the source term to *G*. Inserting this into eq. (14), changing integration variables to $t_1 \equiv t - \tau_2$ and

$\tau_1 \equiv \tau_2 - \tau$, and introducing eq. (15) yields

$$\overline{p^2} \equiv \frac{1}{2T}\int_{-T}^{T}\int_{-\infty}^{\infty}\iiint_V \gamma_{ij}(\boldsymbol{x}|\boldsymbol{y},t+t_o-\tau)\gamma_{kl}(\boldsymbol{x}|\boldsymbol{y},t-\tau_2)\rho v_i' v_j'(\boldsymbol{y},\tau)\rho v_k' v_l'(\boldsymbol{y}_1,\tau_2)\, d\boldsymbol{y}\, d\boldsymbol{y}_1\, d\tau\, d\tau_2\, dt$$

$$= \int_{-\infty}^{\infty}\iiint_V \gamma_{ij}(\boldsymbol{x}|\boldsymbol{y},t_1+t_o+\tau_1)\,\gamma_{kl}(\boldsymbol{x}|\boldsymbol{y}_1,t_1)R_{ijkl}(\boldsymbol{y};\boldsymbol{y_1}-\boldsymbol{y},\tau_1)\, d\boldsymbol{y}\, d\boldsymbol{y}_1\, dt_1\, d\tau_1 \qquad (A-3)$$

which upon introducing the separation vector

$$\boldsymbol{\eta} \equiv \boldsymbol{y_1} - \boldsymbol{y} \qquad (A-4)$$

can be written more compactly as eq. (13) with

$$\overline{\gamma}_{ijkl}\left(\boldsymbol{x}\middle|\boldsymbol{y};\boldsymbol{\eta},t_0+\tau_0\right)$$
$$\equiv\int_{-\infty}^{\infty}\gamma_{ij}\left(\boldsymbol{x},\boldsymbol{y},t_1+t_o+\tau_o\right)\gamma_{kl}\left(\boldsymbol{x}\middle|\boldsymbol{y}+\boldsymbol{\eta},t_1\right)dt_1$$
$$(\mathrm{A}-5)$$

The quantities $\boldsymbol{y}_1, t_1, \tau_1$ are dummy integration variables and we are using the fact that *G* and therefore γ_{ij} depend on *t* and τ only in the combination $t-\tau$.

Appendix B

Far Field Expansion and Neglect of Retarded Time

Taking Fourier transforms of eq. (12) with respect to $(x_1 - y_1)$ and $(t-\tau)$ shows (since G can depend on these quantities only in these combinations) that

$$\widetilde{\mathcal{L}_k}\overline{G}_o = \frac{\delta(\boldsymbol{x}_\perp - \boldsymbol{y}_\perp)}{(2\pi)^2} \qquad (B-1)$$

where

$$\widetilde{\mathcal{L}_k} \equiv \frac{\partial}{\partial x_j}\frac{\widetilde{c_o^2}}{(kU-\omega)^2}\frac{\partial}{\partial x_j} + 1 - \frac{k^2\widetilde{c_o^2}}{(kU-\omega)^2} \quad j = 2,3 \qquad (B-2)$$

is the reduced Rayleigh operator and

$$\overline{G_o}(\boldsymbol{x}_\perp|\boldsymbol{y}_\perp;k,\omega) \equiv -i\frac{(\omega - U(\boldsymbol{y})k)^3}{(2\pi)^2} \iint e^{-i[k(x_1-y_1)-\omega(t-\tau)]}G(\boldsymbol{x},t|\boldsymbol{y},\tau)\,d(t-\tau)\,d(x_1-y_1) \qquad (B-3)$$

where $\boldsymbol{x}_\perp$ and $\boldsymbol{y}_\perp$ have the obvious meaning. Inserting this into eqs. (21) and (A–2) shows (after some rearrangement) that

$$\Gamma_{ij} = -\left(\delta_{in}\delta_{jm} - \frac{\gamma-1}{2}\delta_{ij}\delta_{nm}\right)\frac{\partial}{\partial y_m}\widetilde{c^2} \int_{-\infty}^{\infty}\frac{1}{(\omega - kU(\boldsymbol{y}_\perp))^2}\frac{\partial}{\partial y_n}e^{ik(x_1-y_1)}\overline{G_o}\,dk - i\delta_{1i}(\gamma-1)\frac{\partial U}{\partial y_j}\int_{-\infty}^{\infty}\frac{e^{ik(x_1-y_1)}\overline{G_o}}{(\omega - kU(\boldsymbol{y}_\perp))}dk \qquad (B-4)$$

This result is much simpler in the far field where $U(\mathbf{x}_\perp) \to 0$, $\widetilde{c_0^2} \to c_\infty^2$ = constant, and

$$\overline{G_o} \to \frac{e^{-x_\perp \sqrt{k^2-(\omega/c_\infty)^2}}}{\sqrt{x_\perp}} \widetilde{\mathcal{G}_0}\left(\varphi, k, \omega \middle| \boldsymbol{y}_\perp\right) \quad \text{as } x_\perp \to \infty \qquad (B-5)$$

Here, $x_\perp \equiv |\mathbf{x}_\perp|$ and $\varphi \equiv \tan^{-1}\frac{x_2}{x_3}$ denotes the circumferential angle. Inserting this into eq. (B–4) and using stationary phase to evaluate the integrals now shows that

$$\begin{aligned}\Gamma_{ij} \to & -\frac{e^{i\omega(x-y_1\cos\theta)/c_\infty}}{x}\sqrt{\frac{2\pi i\omega\sin\theta}{c_\infty}}\,\overline{\Gamma}_{ij}\left(\boldsymbol{x}\middle|\boldsymbol{y}_\perp\right) \equiv \\ & -\frac{e^{i\omega x/c_\infty}}{x}\sqrt{\frac{2\pi i\omega\sin\theta}{c_\infty}}\left[\left(\delta_{in}\delta_{jm}-\frac{\gamma-1}{2}\delta_{ij}\delta_{nm}\right)\right. \\ & \times\frac{\partial}{\partial y_m}\frac{\widetilde{c^2}/\omega^2}{\left[M(\boldsymbol{y}_\perp)\cos\theta-1\right]^2}\frac{\partial}{\partial y_n} \\ & \left.-\frac{i\delta_{1i}(\gamma-1)}{\omega}\frac{\partial U}{\partial y_j}\frac{1}{\left[M(\boldsymbol{y}_\perp)\cos\theta-1\right]}\right] \\ & \times e^{-i\omega y_1\cos\theta/c_\infty}\widetilde{\mathcal{G}_0}\left(\varphi,\frac{\omega}{c_\infty}\cos\theta,\omega\middle|\boldsymbol{y}_\perp\right) \\ & \text{as } x\to\infty \qquad (B-6)\end{aligned}$$

where $x \equiv |\boldsymbol{x}|$ is the radial coordinate, $\theta = \arcsin\left(x_\perp/x\right)$ is the polar angle of the observation point and

$$M \equiv U(\mathbf{y}_\perp)/c_\infty \qquad (B-7)$$

is the "acoustic" Mach number at the source point.

Since eq. (B–1) reduces to Helmholtz's equation when $k = 0$, $\overline{G_o}\left(\boldsymbol{x}_\perp\middle|\boldsymbol{y}_\perp;0,\omega\right)$ is given by[21] (see p. 811)

$$\overline{G_o} = -\frac{i}{4(2\pi)^2}\left(\frac{\omega}{c_\infty}\right)^2 H_o^{(1)}\left(\frac{\omega}{c_\infty}\left|\boldsymbol{x}_\perp - \boldsymbol{y}_\perp\right|\right)$$

$$. \quad \to -\frac{1}{2(2\pi)^3}\left(\frac{\omega}{c_\infty}\right)^2 \sqrt{\frac{2\pi}{\left(\omega/c_\infty\right)x_\perp}}\, e^{i\left(\frac{\omega}{c_\infty}|\boldsymbol{x}_\perp - \boldsymbol{y}_\perp| + \frac{\pi}{4}\right)}$$

$$\text{as } x_\perp \to \infty \qquad (B-8)$$

when $\cos\theta = 0$ and $\widetilde{c_0^2} = c_\infty^2 = \text{constant}$, it follows from eqs. (B–5), (B–6), and (25) that

$$\widetilde{\mathcal{G}_0}\left(\varphi, 0, \omega\left|\boldsymbol{y}_\perp\right.\right)$$

$$= -\frac{e^{i\pi/4}}{2(2\pi)^3}\left(\frac{\omega}{c_\infty}\right)^2 \sqrt{\frac{2\pi c_\infty}{\omega}} e^{-i\omega \mathbf{x}_\perp \cdot \mathbf{y}_\perp / c_\infty x_\perp} \qquad (B-9)$$

and therefore that eq. (28) holds.

Appendix C

Reduction of Correlation Coefficients

It is shown in references 15, 24, and 14 that

$$R_{22} = a + \frac{\eta_3^2}{\eta_\perp}\frac{\partial a}{\partial \eta_\perp} - \frac{\partial^2 b}{\partial \eta_1^2} \qquad (C-1)$$

$$R_{23} = -\frac{\eta_2 \eta_3}{\eta_\perp}\frac{\partial a}{\partial \eta_\perp} \qquad (C-2)$$

$$R_{12} = \frac{\eta_2}{\eta_\perp}\frac{\partial^2 b}{\partial \eta_\perp \partial \eta_1} \qquad (C-3)$$

$$R_{11} = -\frac{1}{\eta_\perp}\frac{\partial}{\partial \eta_\perp}\eta_\perp \frac{\partial b}{\partial \eta_\perp} \qquad (C-4)$$

so that integration with respect to the circumferential coordinate shows that

$$\frac{1}{2\pi}\int_V R_{22}^2 d\boldsymbol{\eta} = \int_{-\infty}^{\infty}\int_o^{\infty}\left[\frac{3}{8}\left(\eta_\perp \frac{\partial a}{\partial \eta_\perp}\right)^2 + \left(\frac{\partial^2 b}{\partial \eta_1^2}\right)^2 - \left(\frac{\partial^2 b}{\partial \eta_1^2}\right)\frac{1}{\eta_\perp}\frac{\partial}{\partial \eta_\perp}\left(\eta_\perp^2 a\right)\right]\eta_\perp \, d\eta_\perp \, d\eta_1 \qquad (C-5)$$

$$\frac{1}{2\pi}\int_V R_{23}^2 d\boldsymbol{\eta} = \frac{1}{8}\int_{-\infty}^{\infty}\int_o^{\infty}\left(\frac{\partial a}{\partial \eta_\perp}\right)^2 \eta_\perp^3 \, d\eta_\perp \, d\eta_1 \qquad (C-6)$$

$$\frac{1}{2\pi}\int_V R_{12}^2 d\boldsymbol{\eta} = \frac{3}{8}\int_{-\infty}^{\infty}\int_0^{\infty}\left(\frac{\partial^2 b}{\partial \eta_1 \partial \eta_\perp}\right)^2 \eta_\perp d\eta_\perp d\eta_1 \qquad (C-7)$$

$$\frac{1}{2\pi}\int_V R_{11}^2 d\boldsymbol{\eta} = \int_{-\infty}^{\infty}\int_o^{\infty}\frac{1}{\eta_\perp^2}\left[\frac{\partial}{\partial \eta_\perp}\left(\eta_\perp \frac{\partial b}{\partial \eta_\perp}\right)\right]^2 \eta_\perp \, d\eta_\perp \, d\eta_1 \qquad (C-8)$$

$$\frac{1}{2\pi}\int_V R_{11}R_{22}\,d\boldsymbol{\eta} = \int_{-\infty}^{\infty}\int_{o}^{\infty}\left[\frac{\partial^2 b}{\partial\eta_1^2} - \frac{1}{2\eta_\perp}\left(\frac{\partial}{\partial\eta_\perp}\eta_\perp^2 a\right)\right]$$
$$\left(\frac{\partial}{\partial\eta_\perp}\eta_\perp\frac{\partial b}{\partial\eta_\perp}\right)d\eta_\perp\, d\eta_1 \qquad (C-9)$$

Inserting eqs. (34) and (35) into these results and integrating over $\eta_\perp$ shows that

$$\frac{\int_V R_{22}^2\, d\boldsymbol{\eta}}{2\pi L_1 L_\perp^2\left(\widetilde{\rho u_1^2}\right)^2} = \frac{3\int_V R_{23}^2\, d\boldsymbol{\eta}}{2\pi L_1 L_\perp^2\left(\widetilde{\rho u_1^2}\right)^2} + O\left(\varepsilon^2\right)$$
$$= \frac{3}{4}r^2\int_{-\infty}^{\infty}\int_{0}^{\infty}\left(\tilde{\eta}_\perp\frac{\partial D}{\partial\tilde{\eta}_\perp}\right)^2\tilde{\eta}_\perp d\tilde{\eta}_\perp d\tilde{\eta}_1 + O\left(\varepsilon^2\right) \qquad (C-10)$$

$$\frac{\int_V R_{12}^2\, d\boldsymbol{\eta}}{2\pi L_1 L_\perp^2\left(\widetilde{\rho u_1^2}\right)^2} = \mathrm{O}\left(\varepsilon^2\right) \qquad (C-11)$$

$$\frac{\int_V R_{11}^2\, d\boldsymbol{\eta}}{2\pi L_1 L_\perp^2\left(\widetilde{\rho u_1^2}\right)^2}$$
$$= \frac{1}{8}\int_{-\infty}^{\infty}\int_{0}^{\infty}\bar{B}^2\tilde{\eta}_\perp d\tilde{\eta}_\perp d\tilde{\eta}_1 + O\left(\varepsilon^2\right) \qquad (C-12)$$

$$\frac{\int_V R_{11}R_{22}\, d\boldsymbol{\eta}}{2\pi L_1 L_\perp^2\left(\widetilde{\rho u_1^2}\right)^2}$$
$$= \frac{r}{2}\int_{-\infty}^{\infty}\int_{0}^{\infty}\bar{B}\left(\frac{\partial}{\partial\tilde{\eta}_\perp}\tilde{\eta}_\perp{}^2 D\right)d\tilde{\eta}_\perp d\tilde{\eta}_1 + O\left(\varepsilon^2\right) \qquad (C-13)$$

where we have put

$$\bar{B} \equiv -\frac{1}{\bar{\eta}_\perp}\frac{\partial}{\partial\bar{\eta}_\perp}\left(\bar{\eta}_\perp\frac{\partial B}{\partial\bar{\eta}_\perp}\right) \qquad (C-14)$$

and r is defined by eq. (42).

References

[1]Lilley, G.M., "On the Noise from Jets," Noise Mechanism, AGARD–CP–131, 1974, pp. 13.1–13.12.

[2]Balsa, T.F., Gliebe, P.R., Kantola, R.A., Mani, R., Strings, E.J., and Wong II, J.C.F., "High Velocity Jet Noise Source Location and Reduction," FAA Rept. FAA–RD–76–79, 1978.

[3]Khavaran, A., "Role of Anisotropy in Turbulent Mixing Noise," *AIAA Journal*, vol. **37**, no. 7, 1999, pp. 832–841.

[4]Morris, P.J. and Farassat, F., "Acoustic Analogy and Alternative Theories for Jet Noise," *AIAA Journal*, vol. **40**, no. 4, 2002, pp. 671–680.

[5]Tam, C.K.W. and Auriault, L., "Jet Mixing Noise from Fine-Scale Turbulence," *AIAA Journal*, vol. **37**, no. 2, 1999, pp. 145–153.

[6]Goldstein, M.E., "A Generalized Acoustic Analogy," *Journal of Fluid Mechanics*, vol. **488**, 2003, pp. 315–333.

[7]Lilley, G.M., "The Radiated Noise from Isotropic Turbulence with Applications to the Theory of Jet Noise," *Journal of Sound Vibration*, vol. **190**, 1996, pp. 463–476.

[8]Morfey, C.L., Szewczyk, V.M., and Fisher, M.J., "New Scaling Laws for Hot and Cold Jet Mixing Noise Based on a Geometric Acoustics Model," *Journal of Sound and Vibration*, vol. **46**, no. 1, 1976, pp. 79–103.

[9]Freund, J.B., "Noise Sources in a Low-Reynolds-Number Turbulent Jet at Mach 0.9," *Journal of Fluid Mechanics*, vol. **438**, 2001, pp. 277–305.

[10]Freund, J.B., "Noise-source Turbulence Statistics and the Noise from a Mach 0.9 Jet," Phys. of Fluids, Vol. 15, No. 6, 2003, pp. 1788–1800.

[11]Ffowcs William, J.E., " Noise from Turbulence Convected at High Speed," Phil. Trans. Roy. Soc., A **225**, 1963, pp. 469–503.

[12]Goldstein, M.E. and Rosenbaum, B.M., "Emission of Sound from Turbulence Converted by a Parallel Flow in the Presence of Solid Boundaries," NASA TN D–7118, 1973.

[13]Goldstein, M.E. and Rosenbaum, B., "Effect of Anisotropic Turbulence on Aerodynamic Noise," *Journal of the Acoustical Society of America*, vol. **54**, no. 3, 1973, pp. 630–645.

[14]Kerschen, E.J., "Constraints on the Invariant Function of Axisymmetric Turbulence," *AIAA Journal*, vol. **21**, no. 7, 1983, pp. 978–985.

[15]Lindborg, E., "Kinematics of Homogeneous Axisymmetric Turbulence," *Journal of Fluid Mechanics*, vol. 302, 1995, pp. 179–201.

[16]Batchelor, G.K., "Theory of Homogeneous Turbulence," Cambridge University Press, 1953.

[17]Harper-Bourne, M., "Jet Noise Turbulence Measurements," AIAA Paper 2003–3214, 2003.

[18]Lighthill, M.J., "On Sound Generated Aerodynamically: I. General Theory," *Proceedings R. Society Lond.*, A 211, 1952, pp. 564–587.

[19]Lighthill, M.J., "On Sound Generated Aerodynamically: II. Turbulence as a Source of Sound," *Proceedings R. Society Lond.*, A 222, 1954, pp. 1–32.

[20]Pridmore-Brown, "Sound Propagation in a Fluid Flowing Through an Attenuating Duct," *Journal of Fluid Mechanics*, vol. **4**, 1958, pp. 393–406.

[21]Morse, P.M. and Feshbach, H., "Methods of Theoretical Physics," McGraw-Hill, 1953.

[22]Goldstein, M.E., "Aeroacoustics," McGraw-Hill, 1976.

[23]Ribner, H.E., “The Generation of Sound by Turbulent Jets,” Advances in Applied Mechanics (Academic, New York), vol. 8, 1964, pp. 104–182.

[24]Hinze, J.O., “Turbulence,” McGraw-Hill, New York, 1975.

[25]Pope, S.B., “Turbulent Flows,” Cambridge University Press, 2000, p. 144.

[26]Oberhettinger, F. “Fourier Transforms of Distributions and Their Inverses,” Academic Press (New York), 1973.

[27]Khavaran, A., Bridges, J., and Freund, J.B., “A Parametric Study of Fine-Scale Turbulence Mixing Noise,” NASA/TM—2002-211696, 2002.

[28]Lilley, G.M., ”Jet Noise: Classical Theory and Experiments” in Aeroacoustics of Flight Vehicles, H. Hubbard ed., vol. 1 NASA RP–1258, and WRDC TR–90–3052, 1991, pp. 211–289.

[29]Abramowitz, M. and Stegun, I., “Handbook of Mathematical Functions” National Bureau of Standards, 1965.

[30]Tam, C.K.W., Comment on “Acoustic Analogy and Alternative Theories for Jet Noise Prediction,” AIAA Journal, vol. 41, No. 9, pp. 1844–1845, 2003.

[31]Morris, P.J. and Farassat, F., “Reply by the Authors to C.K.W. Tam,” AIAA Journal, vol. 41, No. 9, pp. 1845–1847, 2003.

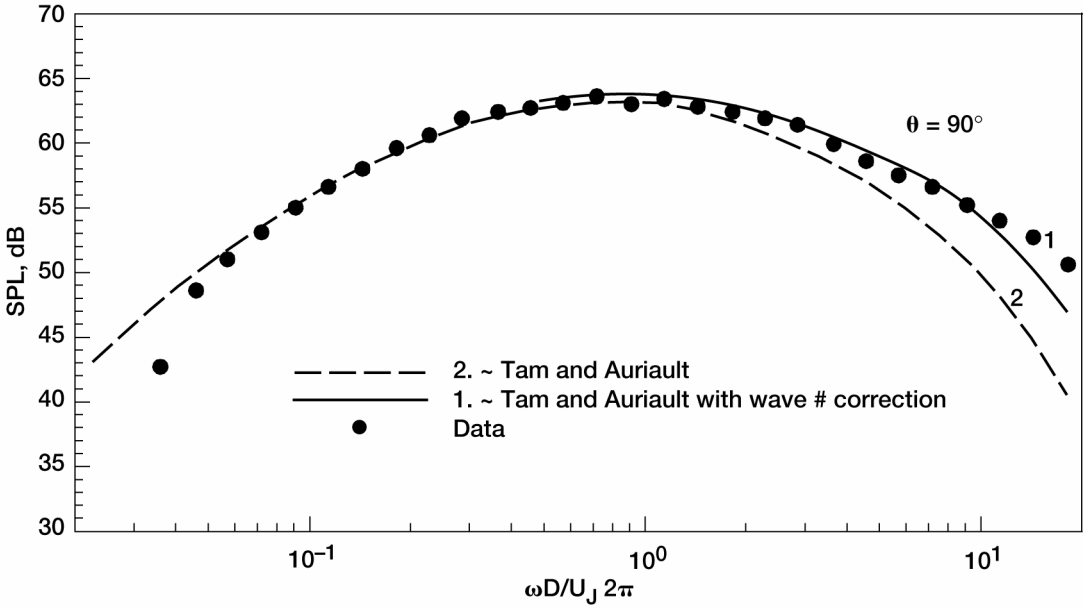

Figure 1.—90° spectal predictions for Mach 0.5 cold jet (based on Ref. 27).